

Subwavelength superfocusing with a dipole-wave-reciprocal binary zone plate

Jun Wang, Fei Qin, Dao Hua Zhang, Dongdong Li, Yueke Wang et al.

Citation: *Appl. Phys. Lett.* **102**, 061103 (2013); doi: 10.1063/1.4791581

View online: <http://dx.doi.org/10.1063/1.4791581>

View Table of Contents: <http://apl.aip.org/resource/1/APPLAB/v102/i6>

Published by the [American Institute of Physics](http://www.aip.org).

Related Articles

One-dimensional broadband phononic crystal filter with unit cells made of two non-uniform impedance-mirrored elements

AIP Advances **3**, 022105 (2013)

Note: Interference effects elimination in wave plates manufacture

Rev. Sci. Instrum. **84**, 016106 (2013)

Color filters for reflective display with wide viewing angle and high reflectivity based on metal dielectric multilayer

Appl. Phys. Lett. **101**, 221120 (2012)

Continuous and scalable fabrication of flexible metamaterial films via roll-to-roll nanoimprint process for broadband plasmonic infrared filters

Appl. Phys. Lett. **101**, 223102 (2012)

Demonstration of an excited-state Faraday anomalous dispersion optical filter at 1529nm by use of an electrodeless discharge rubidium vapor lamp

Appl. Phys. Lett. **101**, 211102 (2012)

Additional information on *Appl. Phys. Lett.*

Journal Homepage: <http://apl.aip.org/>

Journal Information: http://apl.aip.org/about/about_the_journal

Top downloads: http://apl.aip.org/features/most_downloaded

Information for Authors: <http://apl.aip.org/authors>

ADVERTISEMENT

AIP | Applied Physics
Letters

EXPLORE WHAT'S NEW IN APL

SUBMIT YOUR PAPER NOW!

SURFACES AND INTERFACES
Focusing on physical, chemical, biological, structural, optical, magnetic and electrical properties of surfaces and interfaces, and more...

ENERGY CONVERSION AND STORAGE
Focusing on all aspects of static and dynamic energy conversion, energy storage, photovoltaics, solar fuels, batteries, capacitors, thermoelectrics, and more...

Subwavelength superfocusing with a dipole-wave-reciprocal binary zone plate

Jun Wang,^{1,a)} Fei Qin,¹ Dao Hua Zhang,^{1,a)} Dongdong Li,¹ Yueke Wang,¹ Xiaonan Shen,² Ting Yu,² and Jinghua Teng³

¹School of Electrical and Electronic Engineering, Nanyang Technological University, Singapore

²School of Mathematics and Physics Sciences, Nanyang Technological University, Singapore

³Institute of Materials Research and Engineering, Agency for Science, Technology and Research, Singapore

(Received 12 October 2012; accepted 28 January 2013; published online 12 February 2013)

We propose an idea of using a convergent dipole wave at the aperture, radiated from a dipole at distance of z_0 , to produce a perfect focusing at z_0 . We verified this idea through simulation and experimental observation. It is demonstrated that the zone plate designed based on the idea can provide a subwavelength superfocusing by effectively bending the surface waves in a Fresnel region of 100 nm to a couple of wavelengths and is suitable for a situation where a superresolution at a micro working distance is essential. © 2013 American Institute of Physics. [<http://dx.doi.org/10.1063/1.4791581>]

The smallest focal spot¹ circumventing the rule of Abbe's diffraction limit is a fundamental issue in optics. Traditionally, light rays are refracted at a dielectric curved interface and bent towards a focal spot. To go beyond the diffraction limit, focusing at the frequency of visible light has been developed in the field of negative-refractive-index material,² plasmonic structures,³ optical super-oscillation,⁴ etc. Grating coupling of surface plasmon polaritons (SPPs) at an optical wavelength has been explored since 30 years ago.³ In recent years, the plasmonic lenses with subwavelength structures are widely used for focusing and beaming.¹⁻⁶ A perfect focusing can produce a perfect focus like a δ -field distribution in the focus region.^{7,8} With a bandlimited angular spectrum at the aperture with approximation, Merlin proposed a concept of a near field plate for shaping evanescent waves.^{9,10} Despite prior studies on modeling the contribution of evanescent waves to the focus region,^{11,12} there is still lack of a compact plasmonic solution to achieve a perfect focusing.¹³

Significantly, one can obtain a largely enhanced evanescent field when light is transmitted through a subwavelength structure in a metallic thin film. For example, a silver Fresnel zone plate (FZP) is demonstrated to produce higher-frequency spectral information than a dielectric structure.^{14,15} Also, a modified FZP demonstrates a largely reduced depolarization effect in the region of focus and hence offers a better focusing capability.¹⁶ However, the contribution of nonradiative waves to the region of focus is still an obstacle to produce a small focus spot, as it is well known that a FZP is mainly involved in the interference of radiative waves. It is also noted that the interference of surface plasmons excited at the metallic edges forms a sharp focus spot at the center as the two surface waves arrive at the focus after accumulating equal optical paths.¹⁷ From a surface wave focusing (~ 100 nm) to a far-field focusing ($>$ a couple of wavelengths), there is a gap distance for subwavelength superfocusing to be conducted, while in some applications, i.e., nanosensing or nanolithography, a micro

working distance is a need. We expect that the proposed dipole-wave-reciprocal zone plate superlens can fit in these applications.

In this letter, we propose the idea of manipulating a convergent dipole wave-field for a perfect focusing, which is featured by in principle achieving a sharp and strong focus spot. The general idea is further extended to form a binary zone plate to approximate a bandlimited angular spectrum of a dipole wave-field. This proposed zone plate is capable of bending both radiative waves and nonradiative waves and hence is able to bridge a subwavelength superfocusing lens from near field to far field. According to our simulation and experimental studies, this zone plate enables to offer a 300 nm-sized ($\approx 0.47\lambda$) focus spot at the longitudinal distance 600 nm. The zone plate that is designed for 200 nm focusing distance can achieve a focus spot of 193 nm ($\approx 0.30\lambda$). We call the lens a dipole-wave-reciprocal zone plate because the focus spot in the diffraction field takes the role of a dipole source in the radiation field and the sharp and strong focus spot depends on how a dipole wave is represented in reciprocal space.

Let's model a dipole source and its radiation field. A dipole field, radiated from a dipole at the origin, can be expressed as an angular spectrum of plane waves in the form¹⁸

$$\begin{aligned}
 E(k_x, k_y; z) = & \varepsilon \left(\frac{1}{2\pi} \right)^2 \iint_{k_x^2 + k_y^2 \leq k^2} \exp(i(k_x x + k_y y)) \\
 & \times \exp(-i\varepsilon \sqrt{k^2 - k_x^2 - k_y^2} |z|) dk_x dk_y \\
 & + \varepsilon \left(\frac{1}{2\pi} \right)^2 \iint_{k_x^2 + k_y^2 > k^2} \exp(i(k_x x + k_y y)) \\
 & \times \exp(-\sqrt{k_x^2 + k_y^2 - k^2} |z|) dk_x dk_y, \quad (1)
 \end{aligned}$$

where $\varepsilon = +1$ if $z > 0$ and $\varepsilon = -1$ if $z < 0$.
 $k_z = \begin{cases} \sqrt{k^2 - k_x^2 - k_y^2} & \text{if } k_x^2 + k_y^2 \leq k^2 \\ i\sqrt{k_x^2 + k_y^2 - k^2} & \text{if } k_x^2 + k_y^2 > k^2 \end{cases}, \quad k = 2\pi/\lambda.$

^{a)}Authors to whom correspondence should be addressed. Electronic addresses: jwang@pmail.ntu.edu.sg and edhzhang@ntu.edu.sg.

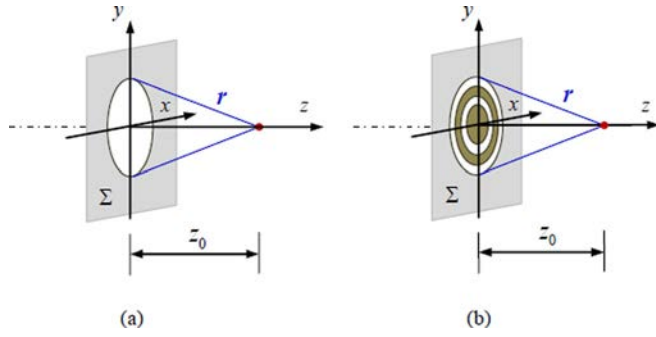


FIG. 1. Schematic of a subwavelength superfocusing based on a convergent dipole wave-field. (a) A convergent dipole wave at the aperture plane Σ ($z=0$), radiated from a dipole located at distance z_0 . (b) Located at the aperture, a zone structure with the properly chosen radii for subwavelength focusing at such distance z_0 .

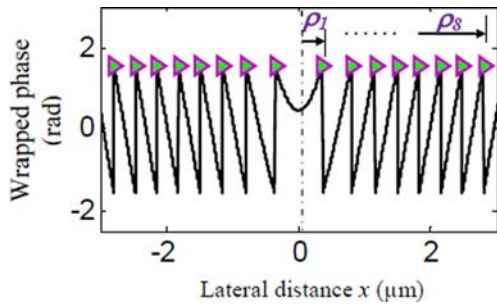


FIG. 2. Design of a binary zone plate according to the wrapped phase distribution of a convergent dipole wave-field.

Hence, as illustrated in Fig. 1(a), a dipole field at the aperture ($z=0$), radiated from a dipole at distance z_0 , is read as

$$\begin{aligned}
 E(k_x, k_y; 0) = & -\left(\frac{1}{2\pi}\right)^2 \iint_{k_x^2 + k_y^2 \leq k^2} \exp(i(k_x x + k_y y)) \\
 & \times \exp\left(i\sqrt{k^2 - k_x^2 - k_y^2}|z_0|\right) dk_x dk_y + \\
 & -\left(\frac{1}{2\pi}\right)^2 \iint_{k_x^2 + k_y^2 > k^2} \exp(i(k_x x + k_y y)) \\
 & \times \exp\left(-\sqrt{k_x^2 + k_y^2 - k^2}|z_0|\right) dk_x dk_y. \quad (2)
 \end{aligned}$$

The denotation of a convergent wave-field follows that of an incoming wave-field.¹⁹ $\varepsilon = -1$ for $z < 0$. Following Weyl's expansion, this is equivalent to a convergent spherical wave towards z_0 in the form

$$\begin{aligned}
 -\frac{1}{2\pi} \frac{\partial}{\partial z} \left(\frac{\exp(-ikr)}{r} \right) = & -\left(\frac{1}{2\pi}\right)^2 \iint \exp(i(k_x x + k_y y \\
 & + k_z |z_0|)) dk_x dk_y, \quad (3)
 \end{aligned}$$

TABLE I. Parameters of a dipole-wave-reciprocal zone plate designed for $\lambda_{in} = 632.8$ nm and $z_0 = 500$ nm.

Radii (ρ_1 to ρ_{10}) (μm)	0.36	0.793	1.153	1.494	1.825	2.152	2.477	2.799	3.12	3.441
Widths of transparent rings (μm)	0.433		0.341		0.327		0.322		0.321	
Actual widths by SEM (μm)	0.462		0.364		0.350		0.346		0.343	

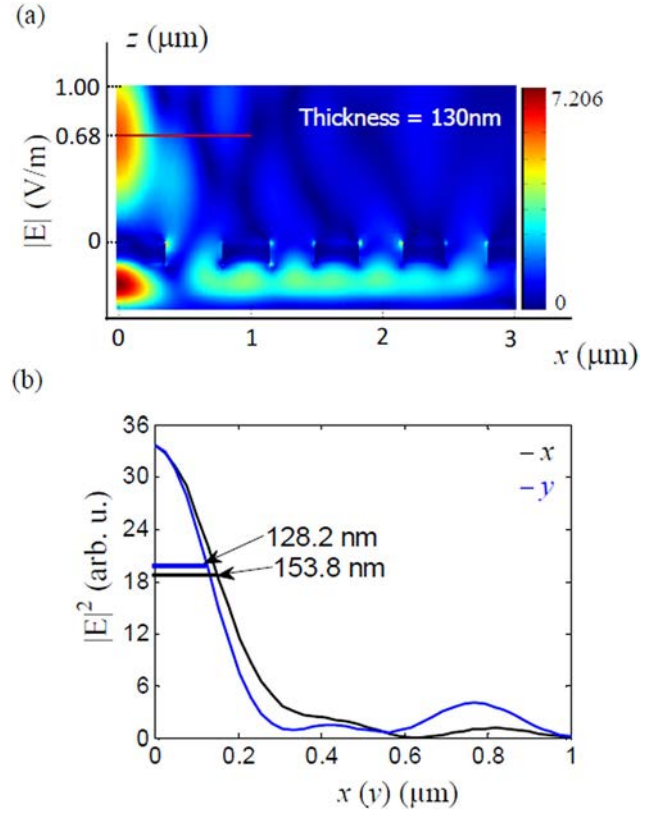


FIG. 3. Simulated subwavelength focusing characteristics with incidence of a p -polarized plane wave, having its electric component parallel to the x direction. (a) Electric field distribution in the x - z plane at $y=0$. (b) Beam profile in the focus region, as indicated in (a), along the x and y lateral directions.

where $r = \sqrt{x^2 + y^2 + z_0^2}$ and k_z is the same as in Eq. (1). In a reciprocal approach,⁶ such convergent field at the aperture can be convergent towards a focus spot at the same distance z_0 .

To validate, a binary zone plate is proposed to approximate the bandlimited angular spectrum of a spherical wave-field (Fig. 1(b)). The radii of transparent and opaque zones are determined by the phase function, $\arg\left(\frac{1}{2\pi} \frac{e^{-ik|r|}}{|r|} \frac{z_0}{|r_i|}\right) \Big|_{\rho_i} = \frac{\pi}{2}$, $|r_i| = \sqrt{(\rho_i^2 + z_0^2)}$. Fig. 2 shows the individual zones with a phase change of $-\pi/2$ to $\pi/2$. The following parameters are used: incident wavelength $\lambda_{in} = 632.8$ nm and focusing distance $z_0 = 500$ nm. The designed radii are tabulated in Table I.

The transmitted wave-field through the structure in gold thin film was simulated using COMSOL Multiphysics, a finite element-based electromagnetic solver. An efficient 3D numerical model was built to simulate one-quarter of the electric field. The dispersive data of gold are adopted from Palik Handbook,²⁰ i.e., at wavelength $\lambda_{in} = 632.8$ nm (frequency $f = c/\lambda_{in} = 473.76$ THz), $\varepsilon_m = -9.371 + 1.095i$. Fig. 3 shows

the COMSOL simulated transmission electric field. The electric intensity distribution in half the x - z plane ($x > 0$) at $y = 0$ shows a focus spot observed at the distance $0.68 \mu\text{m}$ from the aperture ($z = 0$). In the focus region, the size of focus spot achieved can be 307 nm and 256 nm in the x and y directions. The asymmetry of the spot size is attributed to the depolarization effect along the two directions, when the gold structure is incident with p -polarized light.^{21,22}

Experimentally, the proposed zone plate structure with the detailed dimensions shown in Table I has been fabricated by focused ion beam based on an AURIGA CrossBeam (FIB-SEM) workstation of Carl Zeiss. The thin film has an actual thickness of 130 nm on a quartz substrate. As shown in Table I, the slit widths of the fabricated structure are about 7% different from the designed values. To find the effect of a 7% change in slit width on focusing, we did the simulation by keeping the radii, $\rho_1, \rho_3, \rho_5, \dots, \rho_9$ unchanged but varying the radii, $\rho_2, \rho_4, \rho_6, \dots, \rho_{10}$ to produce a 7% increment in all the air widths. It is found that the focusing distance is shifted from $0.68 \mu\text{m}$ to $0.67 \mu\text{m}$, while the FWHM has basically no changes.

With a p -polarized incident plane wave with its electric field component parallel to the x direction, the field intensities at different z positions were measured by a nearfield scanning optical microscope (NTEGRA NSOM of NT-MDT). The probe is with aperture of less than 100 nm . The SEM image of the fabricated plasmonic lens is illustrated in Fig. 4(a); the actual field distributions at different z positions are shown in Figs. 4(b)–4(e); the measured field intensities and the simulated results at different z values are compared in Fig. 4(f), and the focus spot profiles along the x direction are shown in Fig. 4(g). The radii $\rho_1 - \rho_{10}$ as in Table I are the distance from the center to the inner and outer boundaries of the metal zones. The widths of transparent zones are the widths of 5 air rings. For example, the width of the first air ring is $0.433 \mu\text{m}$ which is the difference between ρ_2 and ρ_1 .

It is found that the actual focal spot achieved at $z = 600 \text{ nm}$ is $300 \pm 25 \text{ nm}$ in the x direction, which is adequately smaller than the diffraction limit. The spot size observed is 350 nm at $z = 750 \text{ nm}$ and around 400 nm at the distance up to $z = 1 \mu\text{m}$. This actual focusing distance is within the simulated depth of focus (DOF) that is defined by the FWHM of the central intensity profile along the depth. The higher intensity than the simulated value at 1 micron indicates an elongated DOF and is likely due to the V-shape or U-shape edges of the air slits, formed by Ga^+ -ion-beam bombardments in the fabrication process. Importantly, the experiment results were in good agreement with the simulation results, indicating that the proposed dipole zone plane is reliable to approximate a convergent spherical wavefront.

As a discussion, it is interesting to evaluate any contributions of nonradiative waves in the focus region. The band of the angular spectrum depends on the spatial size of the zone structure with respect to the incident wavelength, where $p^2 + q^2 \leq 1$ representing radiative waves and $1 < p^2 + q^2$ for nonradiative waves.^{23,24} It is believed that if the distance z_0 is as long as many wavelengths, the contribution of evanescent waves is not appreciable.⁷ The contribution to the focus field can be significant when the focusing distance is shorter than one wavelength. Fig. 5 shows the simulation

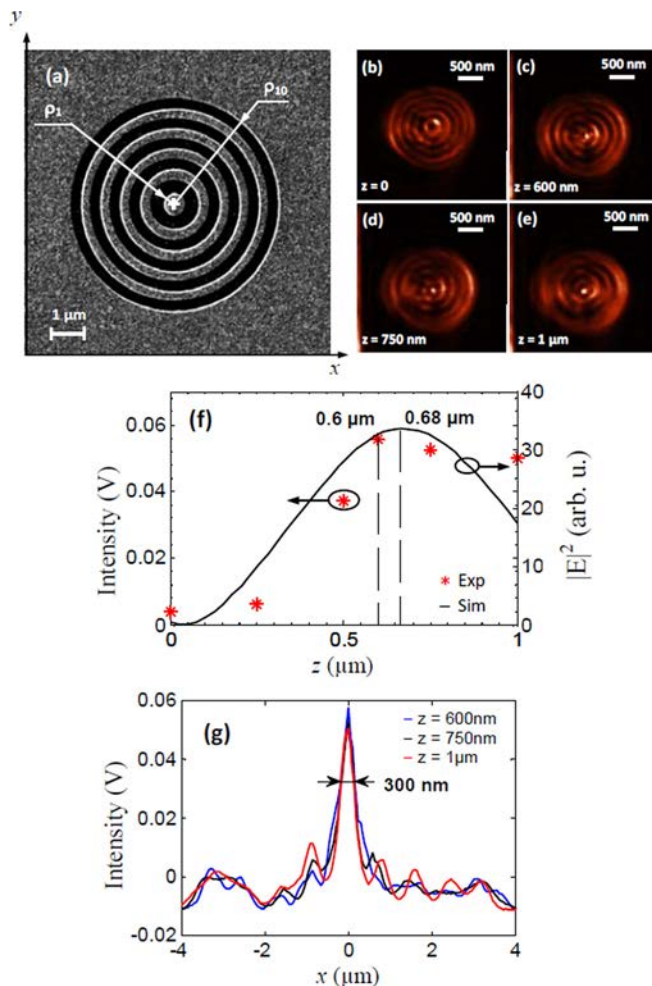


FIG. 4. Experimental characteristics for the same lens as Fig. 3. (a) SEM picture of the superlens, fabricated by focused ion beam. At different longitudinal distances, (b)–(e) electric field intensity distribution observed in the x - y plane, (f) compared intensity in the focus region, and (g) plot of beam profiles along the lateral direction, parallel to the polarization direction. Small focus spot was observed at 600 nm and even at a distance up to $1 \mu\text{m}$.

result for a dipole zone plate, designed with $z_0 = 200 \text{ nm}$, under illumination of a radially polarized plane wave. Due to radial symmetry, the electric field was radially distributed in the x - y plane. The simulation predicts a 193 nm -sized focus spot in the electric near field. Within the distance up to 800 nm , the focus spot size achieved can be $215 \pm 10 \text{ nm}$ in FWHM. The small focus spot can be attributed to the radially symmetric surface waves with a band of k in the focus region.²³ Fig. 5(b) shows the plot of intensity, $|E|^2$ ($=|E_r|^2 + |E_z|^2$), along the longitudinal direction, when one compares the binary zone plate with a Fresnel zone plate. Both zone plates have 317 nm ($\approx 0.5\lambda$) in the width of the outermost zone. It is observed that the intensity maintains its values well in the focus region and also obtains a large enhancement, i.e., a 2.9-fold increase observed at the z distance 500 nm . The observation suggests that the proposed dipole-wave-reciprocal zone plate can bend the surface waves more effectively.

In conclusion, we have investigated subwavelength superfocusing based on an analytical model of a convergent dipole wave, radiated from distance z_0 . The proposed zone plate structure includes a sequence of zones having a phase change of $-\pi/2$ to $\pi/2$. The focusing characteristics was

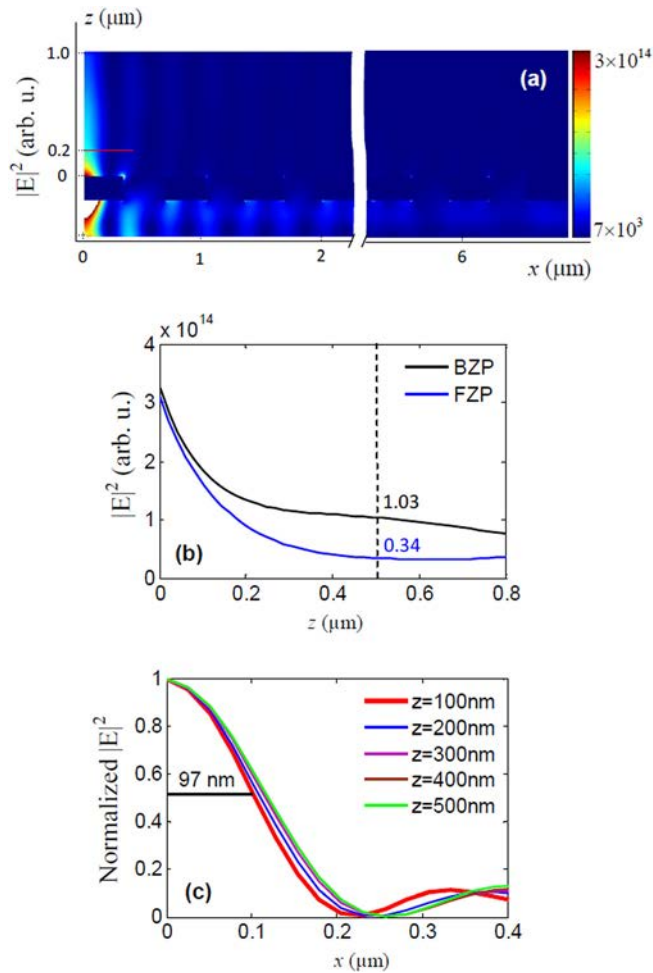


FIG. 5. The COMSOL simulation on a proposed binary zone plate (BZP) with $z_0 = 200$ nm under illumination of a radially polarized plane wave. (a) Electric field intensity distribution observed in the x - z plane at $y=0$, (b) plot of $|E|^2$ along the axial direction at $x=y=0$ and (c) plot of beam profiles along the x direction at different z distances. Compared to a FZP, the proposed zone plate offers considerably enhanced near field in the focus region.

conducted with the parameter $z_0 = 500$ nm. Experimentally, the focus spot size achieved is 300 nm in FWHM at $\lambda_{in} = 632.8$ nm. Significant focusing is found at 600 nm and even at a distance up to $1 \mu\text{m}$ along the z direction. More-

over, to reveal the contribution of surface waves to the focus region, we have compared a binary zone plate with a Fresnel zone plate both using focusing distance $z_0 = 200$ nm. A 2.9-fold enhancement in the electric field in the focus region was observed. It is also noted that the bandlimited angular spectrum is related to the width of the outermost zone.

This project is supported by the Agency for Science and Research (A*Star), under SERC Grant No. 092 154 0099 and National Research Foundation (NRF-G-CPR 2007-01), Singapore. The authors thank Dr. Li Tao for helpful discussions.

¹T. R. M. Sales, *Phys. Rev. Lett.* **81**, 3844–3847 (1998).

²J. B. Pendry, *Phys. Rev. Lett.* **85**, 3966–3969 (2000).

³H. Raether, *Surface Plasmons on Smooth and Rough Surfaces and on Gratings* (Springer, Berlin, 1988).

⁴E. T. F. Rogers, J. Lindberg, T. Roy, S. Savo, J. E. Chad, M. R. Dennis, and N. I. Zheludev, *Nat. Mater.* **11**, 432 (2012).

⁵Y. Q. Fu, J. Wang, and D. H. Zhang, edited by K. Y. Kim, *Plasmonics - Principles and Applications* (InTech, 2012), Chap. 8, pp. 183–228.

⁶B. Lee, S. Kim, H. Kim, and Y. J. Lim, *Prog. Quantum Electron.* **34**, 47–87 (2010).

⁷J. Stamnes, *Opt. Commun.* **37**, 311–314 (1981).

⁸J. Stamnes, *Waves in Focal Regions* (Taylor & Francis Group, 1986).

⁹R. Merlin, *Science* **317**, 927–929 (2007).

¹⁰A. Grbic, L. Jiang, and R. Merlin, *Science* **320**, 511–513 (2008).

¹¹L. E. Helseth, *Opt. Commun.* **281**, 1981–1985 (2008).

¹²L. E. Helseth, *Phys. Rev. A* **78**, 013819 (2008).

¹³H. Shi and L. J. Guo, *Appl. Phys. Lett.* **96**, 141107 (2010).

¹⁴Y. Fu, W. Zhou, L. E. N. Lennie, C. Du, and X. Luo, *Appl. Phys. Lett.* **91**, 061124 (2007).

¹⁵J. H. Li, Y. W. Cheng, Y. C. Chue, C. H. Lin, and T. W. Sheu, *Opt. Express* **17**, 18462 (2009).

¹⁶J. Wang, W. Zhou, E. P. Li, and H. D. Zhang, *Plasmonics* **6**, 269–272 (2011).

¹⁷G. M. Lerman, A. Yanai, and U. Levy, *Nano Lett.* **9**, 2139–2143 (2009).

¹⁸W. H. Carter, *Opt. Commun.* **2**, 142–148 (1970).

¹⁹M. N. Vesperinas, *Opt. Commun.* **67**, 391–395 (1988).

²⁰E. D. Palik, *Handbook of Optical Constants of Solids* (Academic, 1998).

²¹R. G. Mote, S. F. Yu, W. Zhou, and X. F. Li, *Appl. Phys. Lett.* **95**, 191113 (2009).

²²J. Wang, W. Zhou, and A. K. Asundi, *Opt. Express* **17**, 8137 (2009).

²³Z. W. Liu, J. M. Steele, W. Srituravanich, Y. Pikus, C. Sun, and X. Zhang, *Nano Lett.* **5**, 1726 (2005).

²⁴Z. W. Liu, J. M. Steele, H. Lee, and X. Zhang, *Appl. Phys. Lett.* **88**, 171108 (2006).